PERGAMON

Pattern Recognition 35 (2002) 1571–1582

PATTERN RECOGNITION
THE JOURNAL OF THE PATTERN RECOGNITION SOCIETY

www.elsevier.com/locate/patcog

Multiscale skeletons by image foresting transform and its application to neuromorphometry

A.X. Falcão[a,*], L. da Fontoura Costa[b], B.S. da Cunha[a]

[a] *Institute of Computing, University of Campinas, Av. Albert Einstein, 1251, CEP 13084-851, Campinas, SP, Brazil*
[b] *Institute of Physics – IFSC, University of Sao Paulo, Caixa Postal 369, CEP 13560-970, Sao Carlos, SP, Brazil*

Received 6 December 2000; accepted 23 July 2001

Abstract

The image foresting transform (IFT) reduces optimal image partition problems based on seed pixels to a shortest-path forest problem in a graph, whose solution can be obtained in linear time. Such a strategy has allowed a unified and efficient approach to the design of image processing operators, such as edge tracking, region growing, watershed transforms, distance transforms, and connected filters. This paper presents a fast and simple method based on the IFT to compute multiscale skeletons and shape reconstructions without border shifting. The method also generates one-pixel-wide connected skeletons and the skeleton by influence zones, simultaneously, for objects of arbitrary topologies. The results of the work are illustrated with respect to skeleton quality, execution time, and its application to neuromorphometry.

Keywords: Multiscale skeletons; Shape filtering; Image analysis; Image foresting transform; Euclidean distance transform; Exact dilations; Label propagation; Neuromorphometry; Graph algorithms

1. Introduction

In image processing and analysis, many problems can be interpreted as an optimal image partition problem based on seed pixels, where each seed defines a respective influence zone. Such problems can be reduced to a shortest-path forest problem in a graph, whose solution can be obtained in linear time. The method is called *image foresting transform* (IFT) and it has been successfully applied to image segmentation, distance transform computation, and connected filtering [1–3].

Skeletons generation and shape filtering constitute two of the most challenging issues in computer vision and image analysis. The main problems have been to guarantee topology preservation, one-pixel-wide connected skeletons, and shape filtering without border shifting, the latter being a problem typically verified in linear multiscale approaches, such as those based on Gaussian filters. Recently, these problems were circumvented in a single method based on exact dilations to propagate labels assigned to the original contour, producing multiscale skeletons [4]. By varying a threshold value, a family of multiresolution reconstructions of the original shape can be obtained that implements a non-linear filtering of the shape. Such a filtering is characterized by the progressive removal of small-scale details while not affecting more stable portions of the shape. However, the time taken to compute the exact dilations and label propagation using the algorithm described in Ref. [4] is excessive even for images of modest sizes.

The current paper extends the application of the IFT to effectively create multiscale skeletons based on the aforementioned method. The main advantage of such an

* Corresponding author. Tel.: +55-19-3788-5881; fax: +55-19-3788-5847.
E-mail addresses: afalcao@ic.unicamp.br (A.X. Falcão), luciano@if.sc.usp.br (L. da Fontoura Costa), brunosc@ic.unicamp.br (B.S. da Cunha).

0031-3203/02/$22.00
PII: S0031-3203(01)00148-0

approach is to integrate yet another practical and important image analysis tool within the IFT framework. In addition to retaining all the remarkable properties of the original approach, the IFT typically allows about 100 times faster multiscale skeletons generation, and even higher speed-ups can be achieved for larger images. Other results reported in this work include the simultaneous computation of the skeleton by influence zones (SKIZ) [5] and the multiscale skeletons for objects of arbitrary topologies. This involves a simple change in the IFT-based Euclidean distance transform to propagate two types of labels, one used to compute the SKIZ and another to obtain the multiscale skeletons. [1]

In addition to presenting the above-outlined approach to effective multiscale skeletons generation, the current article also addresses how the IFT framework can be applied to solve a series of relevant issues in neuromorphometry, namely the analysis of the geometry of neural cells [7–10]. A growing mass of experimental findings have indicated that the behavior of neural cells and structures can be strongly affected and defined by their respective morphology [11–14]. Here, it is shown how the multiscale skeletonization framework can be effectively used not only to define the area of influence of chicken ganglion retinal cells, but also to characterize their hierarchical structure. Indeed, the high velocity of the reported implementation has paved the way to data mining approaches aimed at investigating general and specific properties of the relationship between the neural shape and function by taking into account large number of neural cells.

This paper is organized as follows. It starts by reviewing the principles underlying the IFT with an example of how it computes the Euclidean distance map. We then describe how this framework can be used to quickly compute both multiscale skeletons and SKIZ simultaneously, including the respective linear-time algorithm. Experimental evaluation of quality and speed as well as its application to neuromorphometry are subsequently covered. We conclude by outlining the main results and the possibilities for future work.

2. An overview of the image foresting transform

Consider the problem of partitioning an image based on seed pixels such that each seed should define a respective influence zone composed of pixels whose "distance" to that seed is minimum. A naive method to solve this problem is to compute and compare the "distance" between each pixel and each seed. A more effective method is to propagate the "distance" values from each seed, simultaneously, until the influence zones of the seeds collide and leave the above comparison for the pixels that participate in this collision. Such a strategy is naturally adopted in the IFT.

The IFT maps an image into a graph, computes a shortest-path forest in the graph, and outputs an *annotated image*, which basically represents the associated forest. This process requires to think the image as a graph, where the pixels are the nodes of the graph and the arcs are defined by an *adjacency relation* between pixels. A path in the graph is a sequence of adjacent pixels. The "distance" from a seed to a pixel is defined as the "length" of the shortest-path from the seed to the pixel in this graph. Such a "distance" is found by minimizing a suitable *path-function*, pf. The choice of the adjacency relation and the path-function depends on the nature of the problem. For example, assume that two pixels p and q are said adjacent if

$$d(p,q) \leqslant R, \tag{1}$$

where $d(p,q)$ is the Euclidean distance between p and q and R is a positive number. In a region-based image segmentation problem, for instance, one could choose the 4-neighborhood relation ($R = 1$) and the path-function as a mapping that assigns to each path in the graph its highest arc weight, where the weight of an arc is the absolute difference between the brightness of its adjacent pixels.

In addition to the parameters that define a graph, a label may also be assigned to each seed pixel. Thus, the IFT grows a shortest-path tree, simultaneously, from each seed in the graph, propagating the following properties to each pixel in the annotated image: the label of its closest seed, the "distance" from its closest seed, and the parent pixel that leads it back to its closest seed. At least one of these properties should be relevant for a given problem. For example, image segmentation based on region growing and watershed transforms, output the label image that represents the influence zones of all seeds in the optimal image partition. Distance transforms and connected operators output the "distance" image, which represents a distance map in the former and a gray-scale image in the latter. The parent pixel has been used for image segmentation based on edge tracking and geodesic path computation.

To complete this overview about the IFT, let us consider the problem of partitioning an image based on two seed pixels s and s' such that the influence zone of each seed is defined by the pixels whose Euclidean distance to that seed is minimum. For simplicity, assume the 4-neighborhood relation as shown in Fig. 1a. The

[1] A preliminary version of part of this work is presented in Ref. [6]. The work presented here further describes an experimental evaluation of the method for a real application (neuromorphometry).

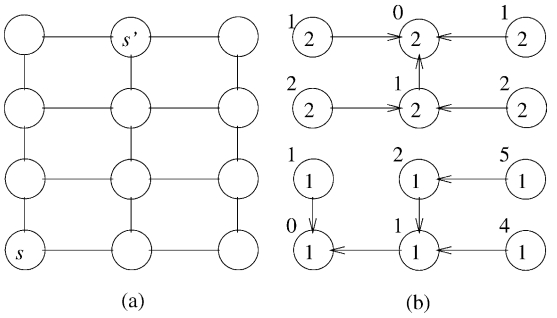

Fig. 1. (a) An image as a graph, where the pixels are the nodes of the graph and the arcs are defined by a 4-neighborhood relation. (b) A shortest-path forest with trees rooted at pixels s and s' of (a) computed based on Eq. (2).

path-function is defined as

$$pf(P) = \left(\sum_{i=1}^{n-1} |x_{p_i} - x_{p_{i+1}}|\right)^2 + \left(\sum_{i=1}^{n-1} |y_{p_i} - y_{p_{i+1}}|\right)^2, \tag{2}$$

where $P = \langle p_1, p_2, \ldots, p_n \rangle$ is a path in the graph and (x_{p_i}, y_{p_i}) are the (x, y) coordinates of a pixel p_i in the image. Fig. 1b presents a shortest-path forest computed based on Eq. (2) when label 1 is assigned to s and label 2 is assigned to s'. The parent pixel is represented by the orientation of the arrows and the propagated labels are written inside the circles. Notice that the "distance" between each pixel and its closest seed in this example is the squared Euclidean distance, which is written outside the circles.

Cuisenaire and Macq use a similar approach to compute the Euclidean distance map [15]. They noticed that there is a relationship between the minimum value of R in Eq. (1) and the size of the image to guarantee exact Euclidean distance values. However, the influence zones of the seeds might not be connected for values of $R > \sqrt{2}$, and so the skeletons. The presented approach uses the 8-neighborhood relation ($R = \sqrt{2}$) to guarantee connected skeletons, and as illustrated in this paper, it is also sufficient to obtain exact Euclidean distance maps in practical situations.

The collision between the influence zones of s and s' is represented by a label transition shown in Fig. 1b. Then, if s and s' are pixels of the same contour in the image, such a label transition contains the points of the skeleton. If s and s' belong to different contours, the label transition contains the points of the SKIZ. Therefore, one can conclude that simultaneous SKIZ and multiscale skeletons generation requires propagation of two types of labels by the IFT: a *contour label* and a *pixel label*. While the former identifies the closest connected contour, the latter indicates the closest pixel in that contour. The result will show two types of label transitions and the next section describes how to create multiscale skeletons and SKIZ from such label transitions.

3. SKIZ and multiscale skeletons generation by IFT

The multiscale skeletonization method described in this section is based on the method proposed in Ref. [4]. In addition to the more expedite processing allowed by the IFT, the currently described approach also incorporates the SKIZ concept introduced by Lantuejoul and Beucher [5] in order to cope with images containing more than a single connected component or object, but here the exact distance guarantees a high accuracy and isotropy in defining the frontiers of the obtained domains.

Fig. 2 illustrates the whole process of creating SKIZ and multiscale skeletons, and the multiscale shape filtering by reconstructing the original shapes from the skeletons, SKIZ and the Euclidean distance map. Given a binary image I with multiple objects (e.g. an image with two neurons of a chicken ganglion retinal cell as shown in Fig. 3a), all object pixels that have at least one background pixel as a 4-neighbor are taken as seeds for the IFT, since they represent the pixels of all contours in the image. The strategy for the IFT is to identify and label each of these contours by consecutive integer values. More specifically, all the pixels in the first contour are labeled 1, all the pixels in the second are labeled 2, and so on. Observe that the order in which the contours are numbered is arbitrary, implying only small displacements of one pixel between the obtained frontiers. Such labels are the contour labels defined in the previous section. For each contour, all pixels are also sequentially labeled by increasing integer values while circumscribing the shape, for instance by using the contour tracking algorithm described in Ref. [16]. Observe that the sense (i.e. clockwise or counterclockwise) adopted during this labeling process is arbitrary and has minimal effect over the final results (i.e. some portions of the skeleton can be shifted by one pixel). Such labels are the pixel labels defined in the previous section. Now, the IFT propagates the contour labels, the pixel labels, and the squared Euclidean distance values from each seed as described in the previous section. This process outputs an annotated image which consists of contour labels L_c, pixel labels L_p, and the squared Euclidean distances E (see Fig. 2), and it can be implemented using the algorithm given below.

IFT Algorithm

Input: A binary image $I(p)$;

Output: An annotated image consisting of the contour labels $L_c(p)$, the pixels labels $L_p(p)$ and the squared Euclidean distances $E(p)$;

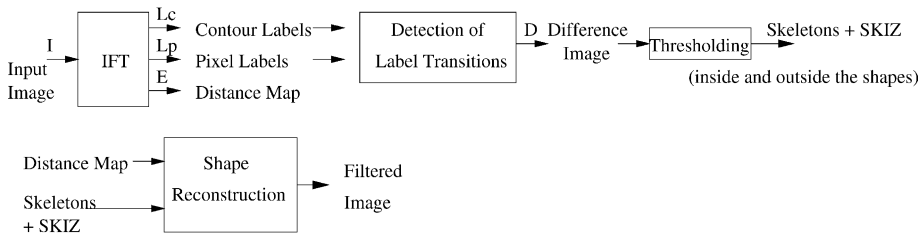

Fig. 2. SKIZ and multiscale skeletons generation by IFT. Shape filtering is obtained from the skeletons, SKIZ, and the Euclidean distance map.

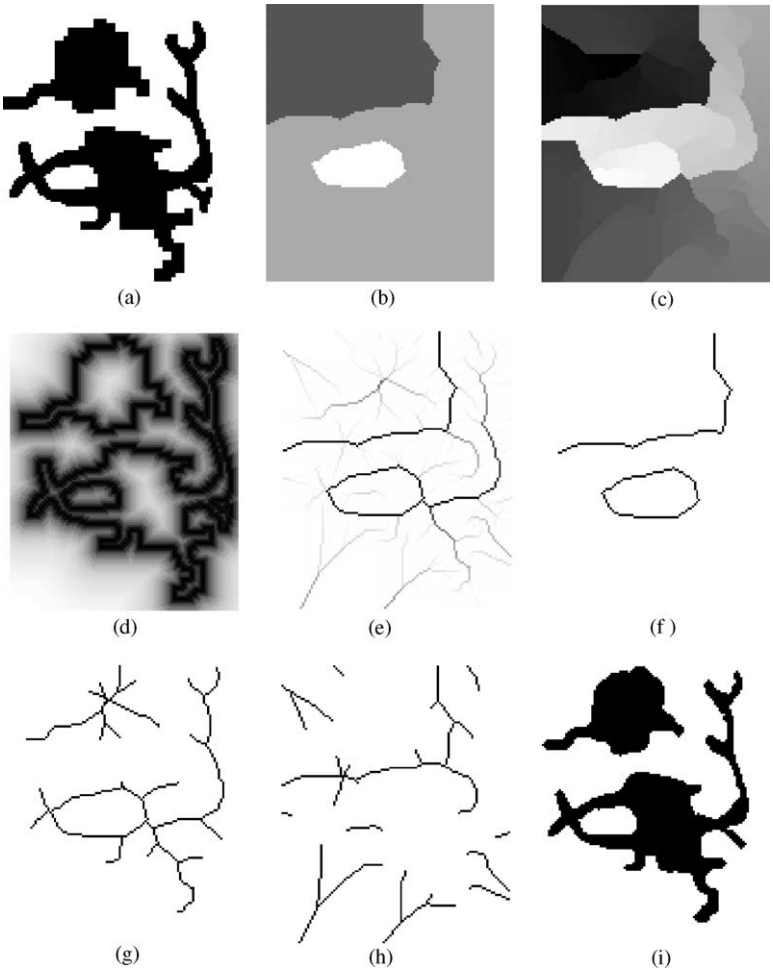

Fig. 3. Images that illustrate the multiscale skeletonization and shape filtering processes shown in Fig. 2. (a) Binary image of two neurons of a chicken ganglion retinal cell. (b)–(d) Contour labels, pixel labels, and Euclidean distances propagated by IFT, respectively. (e) Difference image. (f) SKIZ. (g)–(h) Skeletons and SKIZ inside and outside the shapes, respectively. (i) Filtered image.

Auxiliary data structures: Two 2D arrays $d_x(p)$ and $d_y(p)$ that accumulate the positive increments along x and y directions according to Eq. (2). A priority queue Q. A 2D array $s(p)$ that indicates three possible values for the status of a pixel p in Q: *initial*—p was never inserted in Q; *inserted*—p has been inserted in Q; and *removed*—p has been removed from Q.

begin

(1) for all pixels $p \in I$, which are not contour pixels, set $d_x(p)$ to ∞, $d_y(p)$ to ∞, $E(p)$ to ∞, $L_p(p)$ to 0, $L_c(p)$ to 0, and $s(p)$ to *inicial*;

(2) *for* each contour in I, assign a consecutive integer label, apply a contour following the algorithm that visits each pixel p in that contour and *do*

  (a) set a consecutive integer to $L_p(p)$, the current contour label to $L_c(p)$, $E(p)$ to 0, $d_x(p)$ to 0, and $d_y(p)$ to 0;

  (b) insert p into Q with priority 0 and set $s(p)$ to *inserted*;

(3) *while* $Q \neq \emptyset$ *do*

  (a) remove a pixel p of least priority value from Q and set $s(p)$ to *removed*;

  (b) *for* each pixel q adjacent to p such that $s(q) \neq$ *removed do*

    (i) set tmp to $(d_x(p) + |x_p - x_q|)^2 + (d_y(p) + |y_p - y_q|)^2$, where (x_p, y_p) and (x_q, y_q) are the (x, y) coordinates of p and q in I;

    (ii) *if* $tmp < E(q)$, *then*

      (A) set $d_x(q)$ to $d_x(p) + |x_p - x_q|$, $d_y(q)$ to $d_y(p) + |y_p - y_q|$, $L_p(q)$ to $L_p(p)$, $L_c(q)$ to $L_c(p)$ and $E(q)$ to tmp;

      (B) *if* $s(q) \neq$ *inserted*, *then* insert q in Q with priority $E(q)$ and set $s(q)$ to *inserted*, *else* update the position of q in Q with new priority value $E(q)$;

    end if;

  end for;

end while;

end

The IFT algorithm above is essentially the Dial algorithm [17]. Its linear-time implementation requires a priority queue Q as described in the Dial implementation of the Dijkstra algorithm [18,19].

Note that the seeds (contour pixels) are inserted in Q in the increasing order of contour labels and pixel labels, respectively (item 2 of the algorithm). As a default of all previous implementations of the IFT, the algorithm follows a *first-in first-out* rule for pixels that have the same priority in Q. Therefore, whenever a pixel presents the same Euclidean distance to more than one seed pixel, it keeps the smallest label and this rule is valid for both contour and pixel labels. Such a rule is a condition in Ref. [4] and it is naturally satisfied here.

Figs. 3b–d present the contour labels L_c, the pixel labels L_p, and the Euclidean distance map E computed by the IFT. Continuing the process presented in Fig. 2, label transitions should be detected in order to define a difference image D (Fig. 3e). Such an image is obtained by the following rules applied over each pixel p in D. First, intermediate difference images D_1 and D_2 are computed.

$$D_1(p) \leftarrow \max_{\forall q \in N_4(p)} \{L_c(q) - L_c(p)\}, \tag{3}$$

$$D_2(p) \leftarrow \max_{\forall q \in N_4(p)} \{L_p(q) - L_p(p)\}, \tag{4}$$

where $N_4(p)$ is the set of pixels that are 4-neighbors of p. If $D_1(p) > 0$, then $D_1(p) \leftarrow M$, where M is the maximum label assigned to a pixel in L_p, otherwise $D_1(p) \leftarrow 0$. If $D_2(p) > N/2$, where N is the number of pixels of the contour with label $L_c(p)$, then $D_2(p) \leftarrow N - D_2(p)$. Second, the difference image D is computed as

$$D(p) \leftarrow \max\{D_1(p), D_2(p)\}. \tag{5}$$

Observe that D_1 contains the SKIZ (Fig. 3f), while D_2 encodes label differences related to the skeletons. Now a family of multiresolution skeletons together with the SKIZ can be obtained by thresholding D at the subsequent integer values, which act as the spatial scales. It is also important to observe that two types of skeletons and SKIZ are simultaneously produced by the above-described procedure: those inside (Fig. 3g) and those outside the shapes (Fig. 3h). The higher the threshold value, the more simplified the shapes become, with smaller skeleton detail being progressively removed as the threshold increases. Fig. 4 illustrates this behavior with the skeletons and SKIZ inside the shapes shown in black for six different scales, where the lighter gray shapes are the originals. The obtained skeletons are guaranteed to be connected (topology preservation). In addition, the skeleton segments between branching points and/or extremities are also guaranteed to be one-pixel wide. Observe that it is also possible to use the maximum of the absolute value of the differences in Eqs. (3) and (4), leading to two-pixel wide skeletons and SKIZ segments, respectively. Therefore, the obtained skeletons possess all the relevant properties normally required for medial axis representations. Actually, by having the skeleton of a shape and the distance transform value at each pixel of the skeleton, one can reconstruct the original shape by painting circles centered at each skeleton/SKIZ pixel with radius equal to the corresponding distance transform value at that pixel (see Fig. 3i and the darker gray shapes shown in Fig. 4). Such a reconstruction scheme allows an interesting possibility for shape filtering where its details are removed, as the threshold increases, in such a way that

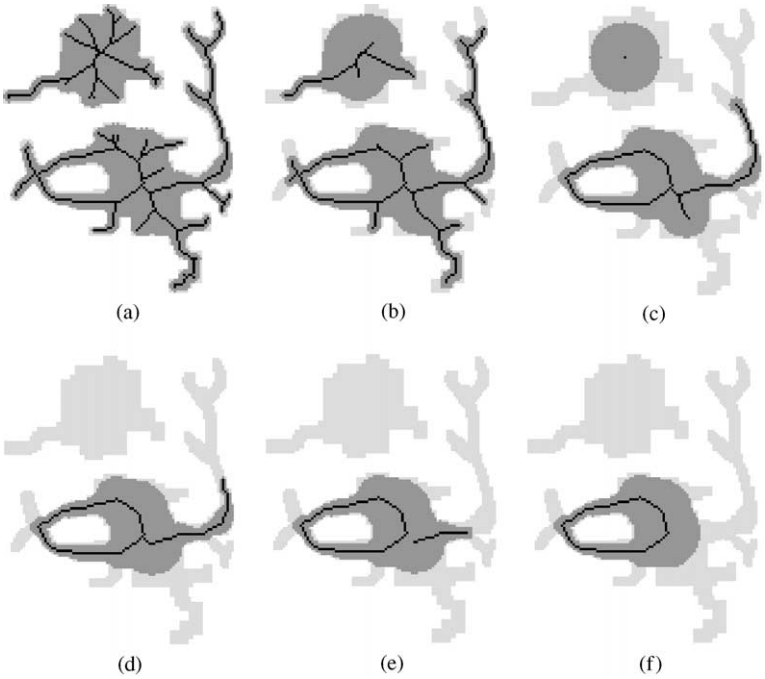

Fig. 4. One-pixel-wide connected skeletons and SKIZ inside the shapes are shown in black for six different spatial scales. The original shapes are shown in lighter gray and the filtered shapes without borders shifting are shown in darker gray.

the position of the borders at more stable regions of the shapes are unaffected, allowing shape filtering without border shifting.

The application of this work with respect to neuromorphometry and its advantages over other methods are presented in the following section.

4. Application to neuromorphometry

The advances of automated imaging verified over the last decade have paved the way to a number of fundamental approaches to the relevant problem of relating neural shape and function. It is now possible to use powerful hardware and increasingly effective algorithms in order to characterize and quantify geometrical aspects underlying neural cells and structures. Basically, a neuron is a specialized cell exhibiting several ramifications (dendrite and axon), which are used for signal transmission and processing. In order to fully understand how a neuron interacts with its environment and neighboring cells, it is necessary to accurately characterize the cell geometry, especially the spatial relationship between adjacent neural cells, as well as the branching pattern underlying each cell. Given its high speed, the just described multiscale skeletonization algorithm, incorporating the SKIZ partitioning of the image space, provides a natural and particularly effective approach to address these two problems, including the possibility of performing data mining over a large number of cells. The great potential of the IFT-based multiscale skeletonization to neuromorphometry is illustrated in the current section. [2]

Consider the gray-level image in Fig. 5, which was obtained by optical microscopy from histological slides of chicken retinal ganglion cells, which are predominantly planar. Since such cells represent the final processing stage in the vertebrate retina, it is important to study how these cells are spatially distributed and adjacent. In addition, the complexity of the dendritic arborizations exhibited by each cell provides further insight about the integration of afferent signals by each cell, which is related to the cell sensitivity. In order to characterize such geometrical issues, each of the neuronal cells in the original image is firstly segmented by using the live-wire-on-the-fly method described in Ref. [19], which allowed an effective, though interactive, means for properly separating each cell and respective arborizations from the cluttered background. [3] The segmented image

[2] A demo of the IFT-based skeletonization method is available in www.ic.unicamp.br/~afalcao. A demo of the original method [4] is available in http://cyvision.if.sc.usp.br/msskeletons.

[3] A demo of the live-wire-on-the-fly method is available in www.mmorph.com/prontomask.

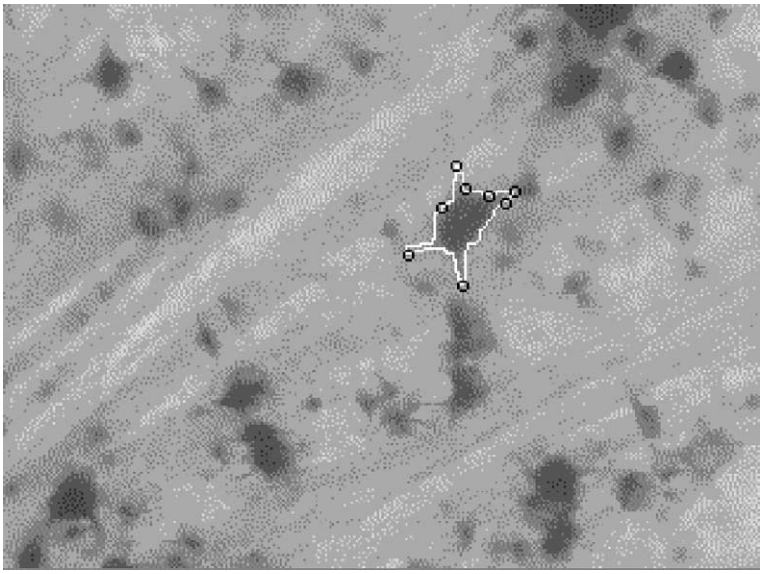

Fig. 5. A gray-level image obtained by optical microscopy from histological slides of chicken retinal ganglion cells.

thus obtained is illustrated in gray in Fig. 6, which also shows the SKIZ partitioning of the considered retinal surface (the tessellation in black), as well as the internal and external skeletons of the cells in each of the areas of influence defined by the SKIZ. It is evident from this figure that the branching pattern of each neuron is clearly captured by the respective internal skeletons, allowing the immediate obtention of the respective dendrograms [20]—a hierarchical data structure describing the cell, which is required by most modern neural simulation approaches.

In addition to the ability to logically partition the retinal space and characterize the branching structures, the IFT-based multiscale skeletonization approach also allows the filtering of each of the neuronal cells in Fig. 6, which is achieved by varying the difference threshold, as illustrated in Fig. 7. Observe that this procedure allows small details in the neural shape to be removed while the borders of the other portions are not shifted, therefore illustrating the potential of the considered framework for shape filtering without border shifting. Such a scale-space representation of the neural cells shown in Fig. 7 allows the identification of the body of each neuronal cell, which is a particularly important neural structure.

Other important feature of the presented method is its robustness to shape rotation and scaling. Such a robustness is crucial for automatic classification of neuron shapes. Figs. 8a–c present an example of the skeleton of a neuron whose shape was rotated to three positions and Fig. 8d illustrates the skeleton computed after scaling the original shape. In all the cases, the threshold that sets the spatial scale was automatically set to 5% of the maximum value in the difference image. Note the high degree of similarity among them.

In the context of this application, the IFT-based skeletonization method was also compared to that proposed by Ogniewicz and Kübler [21], which is based on Voronoi Diagrams. Figs. 6 and 9 show that both methods produce quite similar skeletons and SKIZ. They also run in about the same time.[4] The superior quality of these methods becomes evident when the skeletons are compared to those obtained by morphological skeletonization and morphological thinning [22] (see Fig. 10). Note that the morphological skeletonization cannot guarantee connectedness and morphological thinning cannot eliminate spurious branches.

Finally, the speed of the proposed method has also been compared to that allowed by the original method [4], indicating a clear advantage for the IFT-based skeletonization approach as shown in Table 1. The table shows the execution mean times (in seconds) of the original method and of the proposed method (values in parentheses) to compute the multiscale skeletons of four neurons in images of various sizes. By increasing the size of the image, the execution time for distance and label propagation grows very fast in the original method when the size goes from 240×240 to 300×300 pixels, while the execution time of the proposed method remains less than 1 s. The tests were performed in a PC AMD Athlon, 600 MHz.

[4] The program to generate multiscale skeletons using the Ogniewicz method is available in http://hrl.harvard.edu/people/postdocs/rlo/rlo.dir/rlo-soft.html.

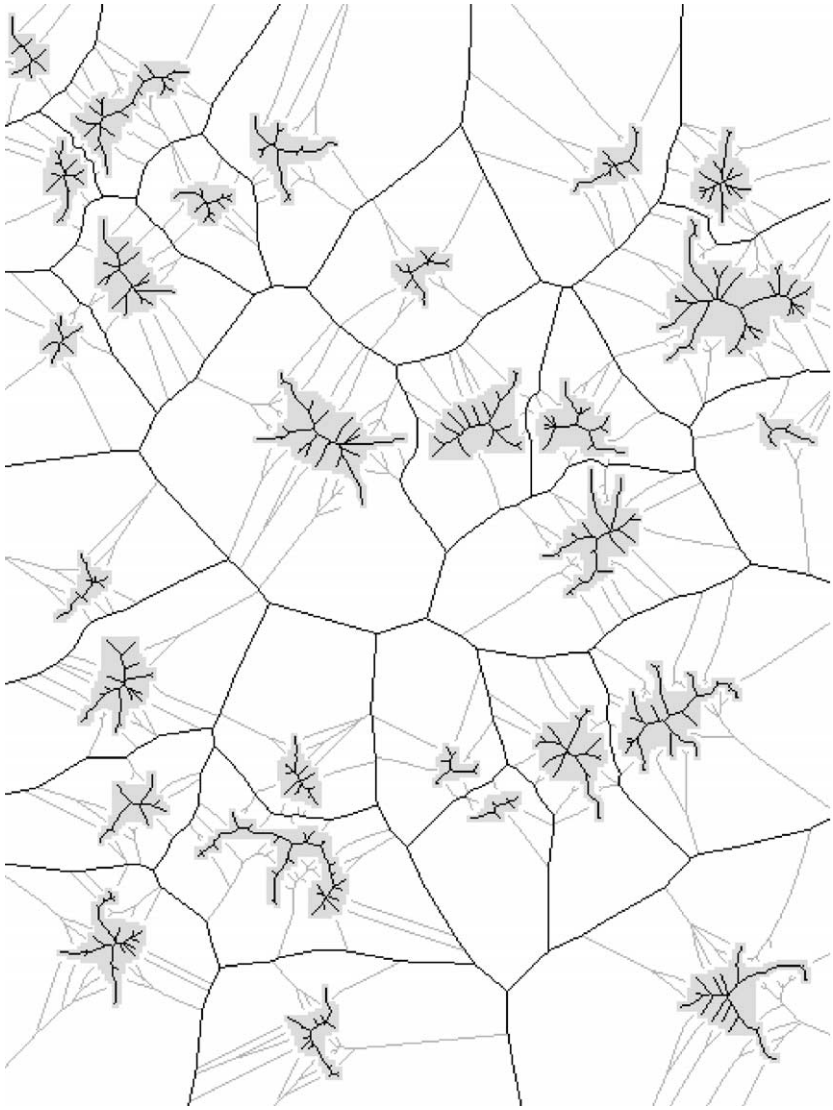

Fig. 6. Segmented image showing skeletons and SKIZ, inside and outside the shapes of some neurons extracted from Fig. 5.

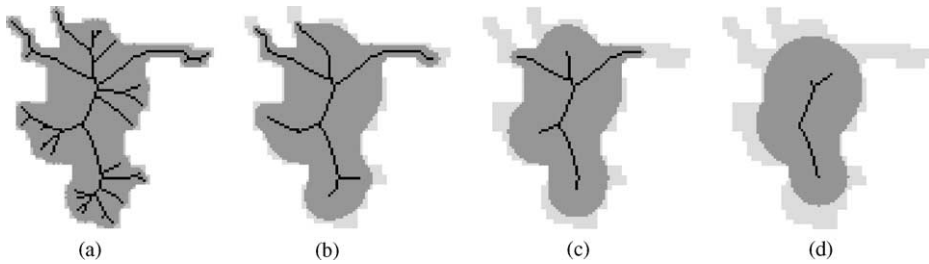

Fig. 7. Scale-space representation of a neural cell. The original shape is shown in lighter gray, the filtered shapes are shown in darker gray, and the skeletons are shown in black.

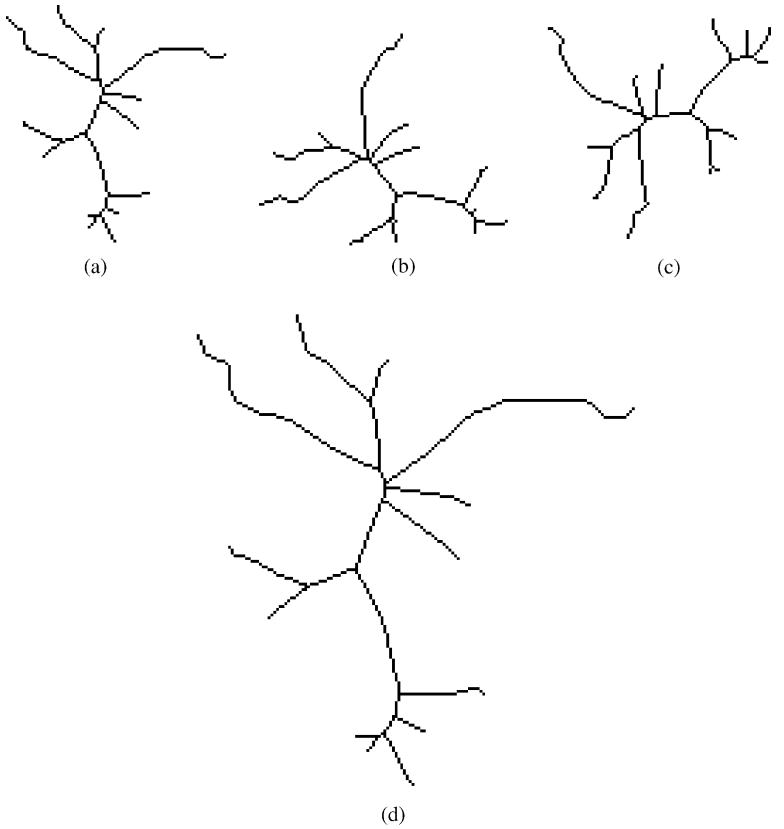

Fig. 8. This example shows the robustness of the presented method to shape rotation and scaling.

5. Conclusion and discussion

This paper has described how the multiscale skeletonization approach originally proposed in Ref. [4] can be naturally and efficiently executed by the IFT, extending the number of techniques implemented within this versatile framework. In addition, it has shown how the SKIZ partitioning of images containing multiple contours can be performed simultaneously with the multiscale skeletonization.

The IFT-based multiscale skeletonization approach has been explained in detail, and the effectiveness of the obtained skeletonization technique has been illustrated with respect to skeleton quality and execution time (compared to other traditional skeletonization approaches). The proposed approach has shown to be much simpler than that presented by Ogniewicz, which is based on Voronoi diagrams [21], and able to produce discrete multiscale skeletons with equivalent high quality in about the same execution time. The superior quality of these methods became evident when the skeletons were compared to those obtained by morphological skeletonization and thinning [22]. The application potential of the proposed approach has also been illustrated in the important and modern problem of neuromorphometry, allowing not only the characterization of the spatial organization of neural structures (such as the distribution of ganglion cells in the vertebrate retina), but also the branching hierarchical structure of each cell.

Currently, the 3D extension of the method is being investigated together with a series of shape descriptors that can be extracted from the multiscale skeletons for object recognition.

Acknowledgements

The work of Alexandre X. Falcão is partially supported by CNPq (Proc. 300698/98-4). Luciano da F. Costa is grateful to CNPq (Proc. 301422/92-3) and FAPESP (Procs. 94/3536-6 and 94/4691-5) for the financial support and to Prof. R. Linden for the kind

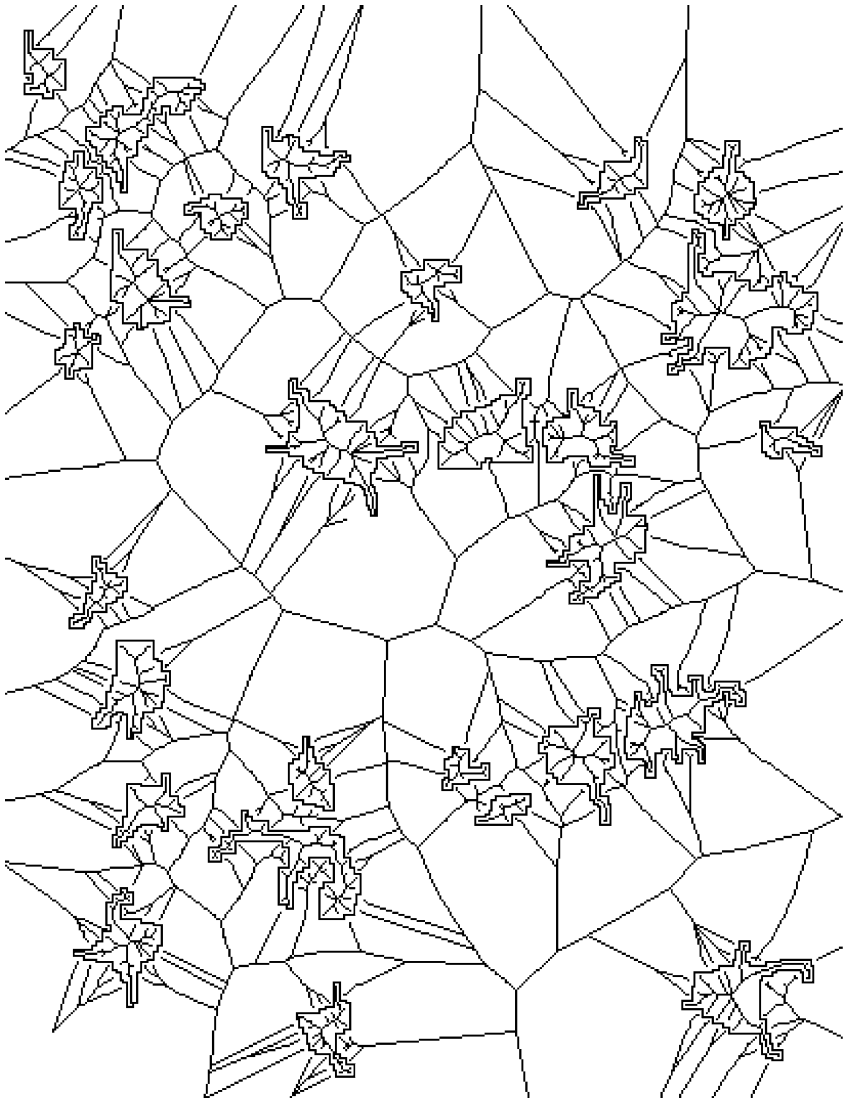

Fig. 9. The same example as shown in Fig. 6, but using the Ogniewicz's method. Note that the IFT-based skeletonization method is simpler and provides the same high-quality skeletons.

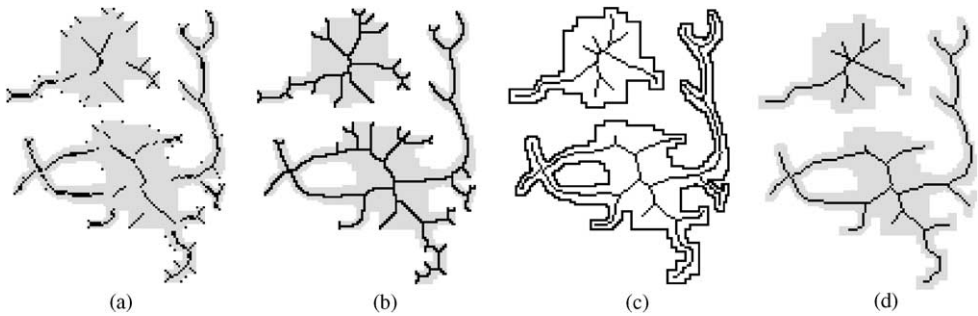

Fig. 10. Skeletons inside the shape computed by (a) morphological skeletonization, (b) morphological thinning, (c) the Ogniewicz's method, and (d) the IFT-based skeletonization method.

Table 1
Execution mean times (in seconds) for computing multiscale skeletons of four neurons in images of various sizes, using the original method [5] and the IFT-based skeletonization method (values in parentheses)

Image size	Neuron 1	Neuron 2	Neuron 3	Neuron 4
100×100	005 (0.081)	004 (0.037)	006 (0.037)	003 (0.055)
140×140	010 (0.102)	009 (0.073)	009 (0.085)	005 (0.088)
180×180	016 (0.129)	015 (0.159)	015 (0.125)	008 (0.132)
220×220	027 (0.338)	026 (0.349)	026 (0.341)	013 (0.328)
240×240	032 (0.277)	029 (0.283)	031 (0.278)	016 (0.298)
300×300	142 (0.618)	138 (0.617)	141 (0.632)	073 (0.602)

supply of histological slides from which the neuron images in this paper were obtained. The work of Bruno S. da Cunha is supported by FAPESP (Proc. 99/10100-3).

References

[1] R.A. Lotufo, A.X. Falcão, The ordered queue and the optimality of the watershed approaches, in: J. Goutsias, L. Vincent, D.S. Bloomberg (Eds.), Mathematical Morphology and its Applications to Image and Signal Processing, Vol. 18, Kluwer Academic Publishers, Palo Alto, USA, June 2000, pp. 341–350.

[2] R.A. Lotufo, A.X. Falcão, F.A. Zampirolli, Fast Euclidean distance transform using a graph-search algorithm, XIII Brazilian Symposium on Computer Graphics and Image Processing, Gramado—RS, Brazil, October 2000, pp. 269–275.

[3] A.X. Falcão, B.S. da Cunha, R.A. Lotufo, Design of connected operators using the image foresting transform, in: M. Sonka, K.M. Hanson, Proceedings of the SPIE on Medical Imaging, Vol. 4322, San Diego, CA, February 2001, pp. 468–479.

[4] L. da F. Costa, L.F. Estrozi, Multiresolution shape representation without border shifting, Electron. Lett. 35 (21) (1999) 1829–1830.

[5] Ch. Lantuéjoul, S. Beucher, On the use of geodesic metric in image analysis, J. Microsc. 121 (1981) 39–49.

[6] A.X. Falcão, B.S. da Cunha, Multiscale shape representation by image foresting transform, in: M. Sonka, K.M. Hanson, Proceedings of the SPIE on Medical Imaging, Vol. 4322, San Diego, CA, February 2001, pp. 1091–1100.

[7] L. da F. Costa, R.C. Coelho, R.M. Cesar Jr., Computer vision based morphometric characterization of neural cells, Rev. Sci. Instrum. 66 (7) (1995) 3770–3773.

[8] L. da F. Costa, R.M. Cesar Jr., R.C. Coelho, Analysis and synthesis of morphologically realistic neural networks, in: R. Poznanski (Ed.), Modeling in the Neuroscience: From Ionic to Neuronal Networks, Academic Press, Harwood, 1999, pp. 505–528 (Chapter 18).

[9] L. da F. Costa, T. Velte, Automatic characterization and classification of ganglion cells from the salamander retina, J. Comparative Neurol. 404 (1) (1999) 33–51.

[10] R.M. Cesar Jr., L. da F. Costa, Application and assessment of multiscale bending energy for morphometric characterization of neural cells, Rev. Sci. Instrum. 68 (5) (1997) 2177–2186.

[11] I. Segev, Sound grounds for computing dendrites, Nature 393 (1998) 207–208.

[12] R.R. Poznanski, Modelling the electronic structure of starbust amacrine cells in the rabbit retina: functional interpretation of dendritic morphology, Bull. Math. Biol. 54 (1992) 905–928.

[13] D.I. Vaney, Territorial organization of direction selective ganglion cells in rabbit retina, J. Neurosci. 14 (1994) 6301–6316.

[14] F. Caserta, E.D. Eldred, E. Fernandez, R.E. Hausman, L.R. Stanford, S.V. Bulderev, S. Schwartzer, H.E. Stanley, Determination of fractal dimension of physiologically characterized neurons in two and three dimensions, J. Neurosci. Methods 56 (1995) 133–144.

[15] O. Cuisenaire, B. Macq, Fast Euclidean distance transformation by propagation using multiple neighborhoods, Comput. Vision Image Understanding 76 (1) (1999) 163–172.

[16] L. da F. Costa, R.M. Cesar Jr., Shape Analysis and Classification: Theory and Practice, CRC Press, Boca Raton, FL, 2000.

[17] R.B. Dial, Shortest-path forest with topological ordering, Commun. ACM 12 (11) (1969) 632–633.

[18] R.K. Ahuja, T.L. Magnanti, J.B. Orlin, Network Flows: Theory, Algorithms and Applications, Prentice-Hall, Englewood Cliffs, NJ, 1993.

[19] A.X. Falcão, J.K. Udupa, F.K. Miyazawa, An ultra-fast user-steered image segmentation paradigm: live-wire-on-the-fly, IEEE Trans. Med. Imaging 19 (1) (2000) 55–62.

[20] L. da F. Costa, A.G. Campos, L.F. Estrozi, L.G. Rios-Filho, A. Bosco, A Biologically-motivated Approach to Image Representation and Its Application to Neuromorphometry, Lecture Notes in Computer Science, Vol. 1811, Seoul, Korea, May 2000, pp. 407–416.

[21] R.L. Ogniewicz, O. Kübler, Hierarchic Voronoi skeletons, Pattern Recognition 28 (3) (1996) 343–359.

[22] J. Barrera, G. Banon, R. de A. Lotufo, R. Hirata Jr., Mmach: a mathematical morphology toolbox for the khoros system, J. Electron. Imaging 7 (1) (1998) 174–210.

About the Author—ALEXANDRE XAVIER FALCÃO received a B.S. in 1988 in Electrical Engineering from the University of Pernambuco, Brazil. He has worked in computer graphics and image processing since 1991. In 1993, he received a M.S. in Electrical Engineering from the University of Campinas, Brazil. During 1994–1996, he worked at University of Pennsylvania on user-steered image segmentation paradigms for his Ph.D. In 1996, he got his doctorate in Electrical Engineering from the University of Campinas, Brazil. He is currently an Assistant Professor at the University of Campinas, Brazil.

About the Author—LUCIANO DA FONTOURA COSTA was born in Sao Carlos (SP, Brazil) in 1962. He got a B.Sc. in Electronic Engineering from the University of Sao Paulo, Brazil (1984), and a Ph.D. degree from King's College, University of London (1992). He has been with the Institute of Physics of the University of Sao Paulo in Sao Carlos since 1985, where he started and has since coordinated the Cybernetic Vision Research Group. Luciano has acted in the editorial board of several journals, including Journal of Real-Time Imaging, Applied Signal Processing, Psyche, and Integrative Neuroscience. He is the author of over 100 international papers and of the book Shape Analysis and Classification (joint authorship with Roberto M. Cesar Jr., CRC Press 2000).

About the Author—BRUNO SANTOS DA CUNHA was born in Brasilia (DF, Brazil) in 1976. In 1998 he received a B.S. in Computer Engineering from the University of Campinas, Brazil. Currently, he attends an M.S. program in Computer Science at the same university.